ELSEVIER

Thermochimica Acta 318 (1998) 143–153

thermochimica acta

Preparation and characterization of coprecipitates and mechanical mixtures of calcium-strontium oxalates using XRD, SEM-EDX and TG

E. Knaepen[a], M.K. Van Bael[a], I. Schildermans[a], R. Nouwen[a], J. D'Haen[b], M. D'Olieslaeger[b], C. Quaeyhaegens[b], D. Franco[a], J. Yperman[a], J. Mullens[a,*], L.C. Van Poucke[a]

[a] *IMO, Laboratory of Inorganic and Physical Chemistry, Limburgs Universitair Centrum, Building D, B-3590 Diepenbeek, Belgium*
[b] *IMO, Materials Physics Division, Limburgs Universitair Centrum, Building D, B-3590 Diepenbeek, Belgium*

Received 29 September 1997; accepted 18 December 1997

Abstract

In view of the study of the chemistry of the oxalate coprecipitation process for preparing BiSrCaCuO superconductors, the characteristics of oxalates of calcium and strontium in the $Ca(NO_3)_2$–$Sr(NO_3)_2$–HNO_3–H_2O–$(NH_4)_2C_2O_4$ system are investigated. Based on XRD, SEM and TG a comparison between the crystal structure, morphology and thermal decomposition behavior of coprecipitated and physically mixed calcium and strontium oxalates with the same Ca/Sr stoichiometry is made. It is shown that the coprecipitated powders form homogeneous solid solutions of which the crystal structure, morphology and thermal behaviour depend on the Ca/Sr stoichiometry. © 1998 Elsevier Science B.V.

1. Introduction

The preparation of coprecipitated Ca–Sr oxalates is part of the study of the oxalate precursor synthesis of bulk $Bi_2Sr_2CaCu_2O_{8+\delta}$ and $Bi_2Sr_2Ca_2Cu_3O_{10+\delta}$ superconductors by the coprecipitation–filtration technique [1,2].

This 'wet chemical method' provides an intimate mixing of the component elements in solution and, consequently, the production of more homogeneous powders compared to powders obtained by the generally used 'ceramic technique' [3]. The main disadvantages of the conventional 'mechanically mixed-oxide/carbonate' synthesis are microscopic compositional inhomogeneities resulting in long calcination and sintering times, nonuniformity of particle size and shape, and lack of reproducibility. In order to improve the homogeneity of the precursors and, consequently, the ultimate properties of the superconductive materials, various chemical routes (mainly sol–gel [4,5], spray-drying [6] and coprecipitation [1,2]) have received special attention and interest during recent years.

Among the precipitation–filtration techniques, the most used precipitating agent is the oxalate ion [7,8]. Metal oxalates are very suitable precursor powders for superconductive oxides, since they can easily be decomposed into their corresponding oxides [9]. Moreover, some oxalates can form solid solutions. The formation of solid solutions of some multi-metal oxalates has been extensively discussed by Scheule [10] and Fischer et al. [11].

In this paper, we report the preparation, characterization and thermal analysis of coprecipitates and mechanical mixtures of calcium–strontium oxalates with different Ca/Sr ratios, including almost the same

*Corresponding author. E-mail: jmullens@luc.ac.be

PII S0040-6031(98)00339-6

ratios as in the superconductive phases. The aim of this research is to compare the characteristics of the coprecipitated oxalates with the physically mixed oxalates and to investigate the influence of the Ca/Sr ratio on the morphology of the coprecipitated powders. Comparison between coprecipitates and mechanical mixtures having the same Ca/Sr ratio and between mutual coprecipitates with different Ca/Sr ratios are based on XRD, SEM-EDX and TG.

2. Experimental

2.1. Methods and apparatus

The Ca–Sr stoichiometry in the coprecipitated and mechanically mixed powders, which were dissolved in 10% nitric acid, was determined by inductively coupled plasma–atomic emission spectroscopy (ICP-AES) on a Perkin–Elmer Optima 3000DV. The elemental analysis was carried out with emission lines of Ca – 317.933, Ca – 393.366, Ca – 396.847, Sr – 232.235, Sr – 421.552 and Sr – 460.733 nm. The structure and the phase composition of all samples were determined by a Siemens D-5000 powder diffractometer using a Cu X-ray source. The morphology and elemental composition of the individual and binary oxalates were examined by scanning electron microscopy (SEM) measurements and energy dispersive X-ray analysis (EDX) on a Philips XL-30 FEG equipped with an EDX detector with a super-ultrathin window. The acceleration voltage used for the SE (secondary electrons)-images was 5 kV. EDX analysis was carried out with higher acceleration voltage.

The thermal behaviour of the precipitates was investigated by means of a TA Instruments Model 2950 (temperature range: ambient to 1000°C) thermogravimetric analyser in inert Ar atmosphere (50 ml/min) using the following heating-rate scheme: 5°C/min until 300°C, 1°C/min until 500°C and 5°C/min until 900°C.

2.2. Materials

All the chemicals used, $Sr(NO_3)_2$ (Merck p.a.), $Ca(NO_3)_2{\cdot}4H_2O$ (Merck p.a.), $(NH_4)_2C_2O_4{\cdot}H_2O$ (Merck p.a.) and HNO_3 (J.T. Baker) were of high purity (>99.9%). Since $Ca(NO_3)_2{\cdot}4H_2O$ is very hygroscopic, a standard solution was prepared, of which the concentration was determined by an EDTA-titration using eriochrome-T as indicator.

2.3. Preparation of oxalate powders

The Ca–Sr oxalate coprecipitates were prepared in a thermostatted case (25.0±0.2°C) by adding a mixture of nitric acid and an aqueous solution of $Ca(NO_3)_2$ and $Sr(NO_3)_2$ to an aqueous solution of 0.3 M $(NH_4)_2C_2O_4$ by two motor driven burettes (Schott Geräte T100) at the same rate and under continuous stirring. A series of samples was prepared using different concentration ratios Ca^{2+}/Sr^{2+} in the metal nitrate solution which contains 0.67 M nitric acid. The coprecipitates obtained were filtered through an acid resistant 0.45 micron Millipore filter and washed with doubly distilled water. Finally, the powders were dried in air. The individual calcium and strontium oxalates were prepared in the same way as described above. Mechanical mixtures of calcium and strontium oxalate were obtained by mixing the individual precipitated oxalates in a ball-mill for a period of 3 h.

3. Results and discussion

3.1. XRD analysis

XRD measurements were performed to identify the prepared solids. The composition of the samples is given in Table 1.

3.1.1. Coprecipitates

Among the individual precipitated strontium oxalate powders (samples 1, 2), only sample 1 (Table 1) is identified as a single phase, corresponding to the tetragonal $SrC_2O_4{\cdot}2.5H_2O$ phase [12], as shown in Fig. 1(a). Adding $Ca(NO_3)_2$ to the $Sr(NO_3)_2$ starting solution, results in the formation of coprecipitates of composition $Ca_xSr_{1-x}C_2O_4{\cdot}yH_2O$ (Table 1, samples 5 to 13). The x-values, derived from ICP-analysis, are shown in Table 1. The first additions of Ca^{2+} (Table 1, samples 5, 6, 7, 8 and 9) causes a shift in the diffraction lines to higher 2θ angles (Fig. 1(b–f)) compared to the lines of $SrC_2O_4{\cdot}2.5H_2O$ (Fig. 1(a)). This decrease in cell volume can be explained by the partial substitu-

Table 1
Composition of single, coprecipitated and mechanically mixed oxalates: ICP and XRD results

Sample	Metal nitrate solution		ICP-analysis: Ca–Sr ratio	XRD-analysis: phase composition
	$[Sr(NO_3)_2]$	$[Ca(NO_3)_2]$		
Strontium oxalate				
1	0.03726 M			$SrC_2O_4{\cdot}2.5H_2O$
2	0.27160 M			$SrC_2O_4{\cdot}H_2O$ (main fraction)+$SrC_2O_4{\cdot}2.5H_2O$
Calcium oxalate				
3		0.01490 M		$CaC_2O_4{\cdot}H_2O$
4		0.1500 M		$CaC_2O_4{\cdot}H_2O$ (main fraction)+$CaC_2O_4{\cdot}3H_2O$
Coprecipitates				
5	0.03737 M	0.00745 M	$Ca_{0.35}Sr_{0.65}C_2O_4{\cdot}2H_2O$	
6	0.03725 M	0.01490 M	$Ca_{0.49}Sr_{0.51}C_2O_4{\cdot}2H_2O$	
7	0.03806 M	0.02235 M	$Ca_{0.56}Sr_{0.44}C_2O_4{\cdot}2H_2O$	$Ca_xSr_{1-x}C_2O_4{\cdot}yH_2O$ solid solution
8	0.03728 M	0.02979 M	$Ca_{0.62}Sr_{0.38}C_2O_4{\cdot}2H_2O$	substitution of Sr by Ca in the lattice of $SrC_2O_4{\cdot}2.5H_2O$
9	0.03728 M	0.03517 M	$Ca_{0.66}Sr_{0.34}C_2O_4{\cdot}2H_2O$	
10	0.03725 M	0.05960 M	$Ca_{0.74}Sr_{0.26}C_2O_4{\cdot}1.7H_2O$	two-phase region mixture of two solid solutions
11	0.03816 M	0.10346 M	$Ca_{0.81}Sr_{0.19}C_2O_4{\cdot}1.5H_2O$	substitution of Ca by Sr in the lattice of $CaC_2O_4{\cdot}1H_2O$
12	0.03727 M	0.12758 M	$Ca_{0.85}Sr_{0.15}C_2O_4{\cdot}H_2O$	
13	0.03728 M	0.16554 M	$Ca_{0.89}Sr_{0.11}C_2O_4{\cdot}H_2O$	
Mechanical mixtures				
14	0.2 g sample 2+0.0833 g sample 4		Ca/Sr=0.35/0.65	XRD pattern of sample 2+sample 4
15	0.2 g sample 2+0.1450 g sample 4		Ca/Sr=0.49/0.51	XRD pattern of sample 2+sample 4

tion of Sr^{2+} (1.12 Å) by Ca^{2+} (0.99 Å) in the lattice of $SrC_2O_4{\cdot}2.5H_2O$. For samples 10 and 11 (Fig. 1(g) and (h)), an additional phase is detected of which the diffraction lines are shifted to lower 2θ angles compared to the lattice of $CaC_2O_4{\cdot}H_2O$ (Fig. 1(k)) [13]. Ultimately, the solubility limit of Ca^{2+} in the $SrC_2O_4{\cdot}2.5H_2O$ lattice is reached and further additions of Ca^{2+} (Table 1, samples 12 and 13) leads to the formation of the $CaC_2O_4{\cdot}H_2O$ single phase, in which some Ca^{2+} is substituted by Sr^{2+}, thus causing an increase in cell volume (Fig. 1(i) and (j)). Fig. 1(k) shows the XRD pattern of individual precipitated calcium oxalate (Table 1, sample 3), identified as monoclinic $CaC_2O_4{\cdot}H_2O$.

3.1.2. Mechanical mixtures

The physical mixtures were prepared by grinding together individually precipitated strontium oxalate and calcium oxalate. In order to mill a sufficient amount of these mixtures, the single oxalates were precipitated, starting from a higher concentration of the metal nitrate solution (Table 1, samples 2 and 4). From XRD results (Fig. 2(a) and (b)) it can be concluded that strontium oxalate and calcium oxalate consists of two phases: sample 2 being a mixture of $SrC_2O_4{\cdot}H_2O$ [13] and $SrC_2O_4{\cdot}2.5H_2O$, sample 4 being a mixture of $CaC_2O_4{\cdot}H_2O$ [13] and $CaC_2O_4{\cdot}3H_2O$ [13]. Appropriate amounts of both solids were weighed out in order to form mechanical mixtures (Table 1: samples 14 and 15) of the same stoichiometry as in the coprecipitated samples 5 and 6. Comparison of the XRD patterns of samples 14 (Fig. 2(c)) and 15 (Fig. 2(d)) with those of samples 2 and 4, demonstrates that all the lines of the two individual oxalate patterns (Fig. 2(a) and (b)) are present: the mixtures with Ca/Sr ratio equal to 0.35/0.65 and 0.49/0.51 contain the same diffraction lines at the same positions, but the relative intensities of the two patterns is changed, due to a change in total composition.

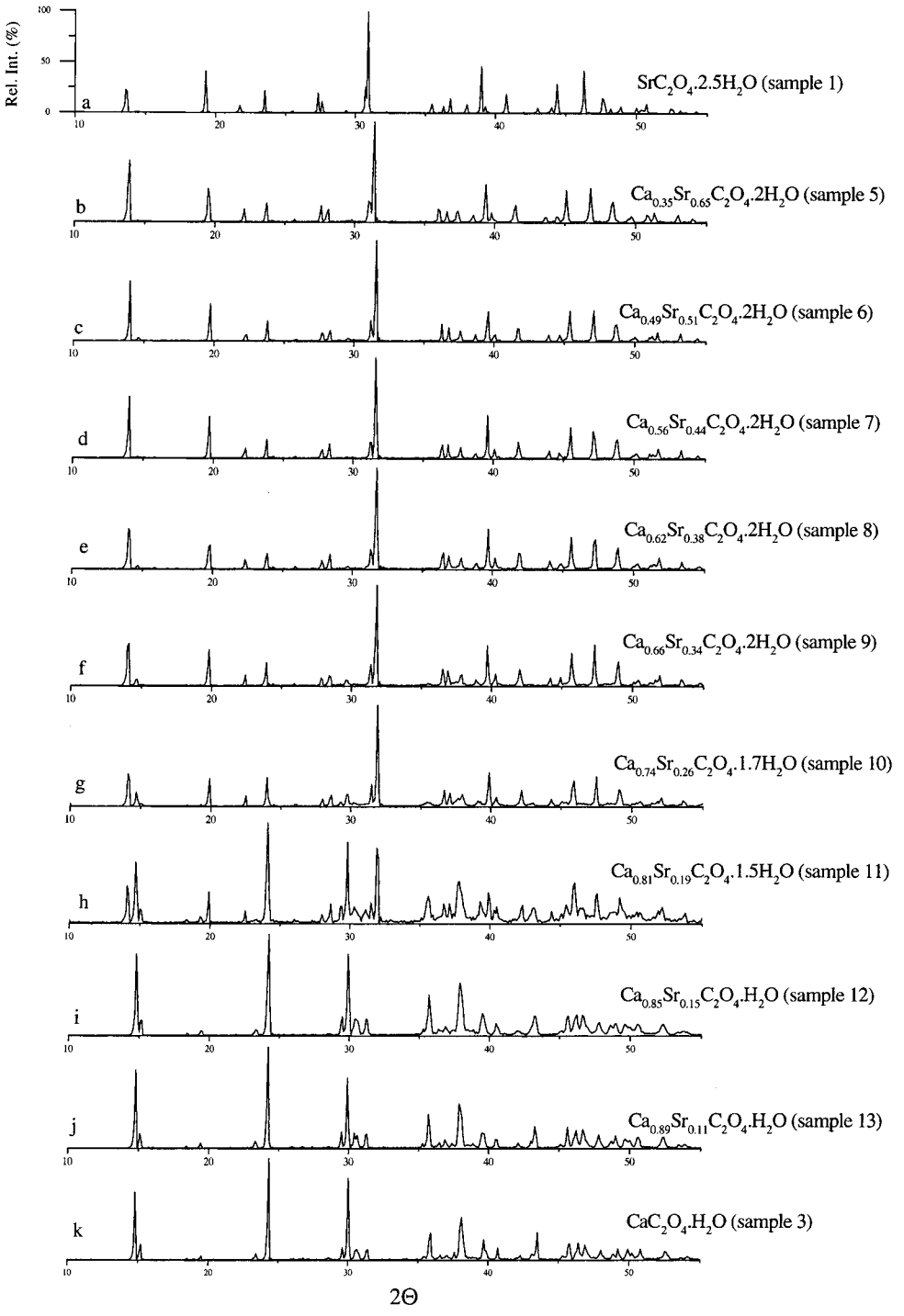

Fig. 1. XRD patterns of the (co)precipitated samples: (a), sample 1; (b), sample 5; (c), sample 6; (d), sample 7; (e), sample 8; (f), sample 9; (g), sample 10; (h), sample 11; (i), sample 12; (j), sample 13; and (k) sample 3.

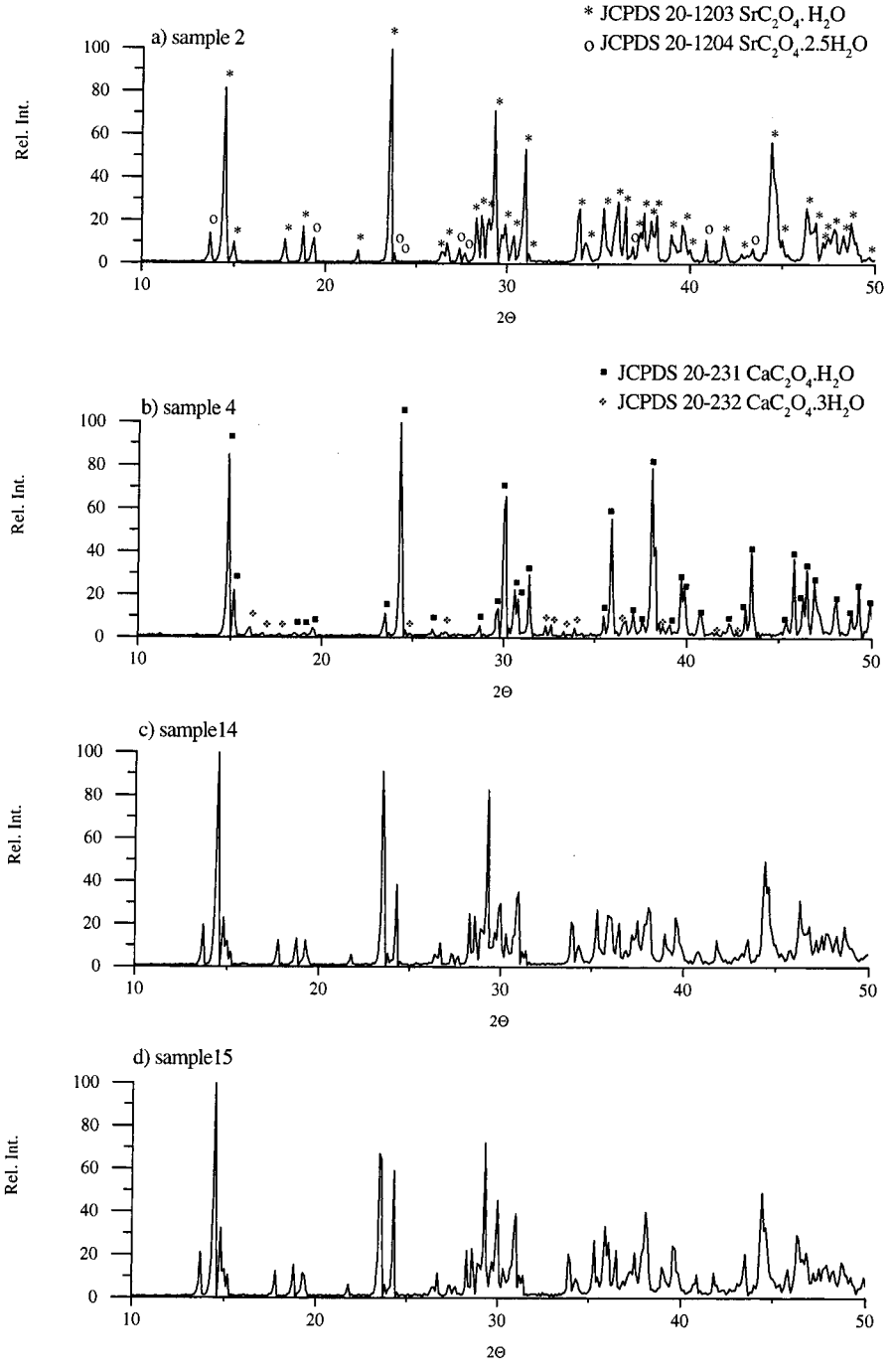

Fig. 2. XRD patterns of individual oxalates and their mechanical mixtures: (a) sample 2; (b) sample 4; (c) sample 14; and (d) sample 15.

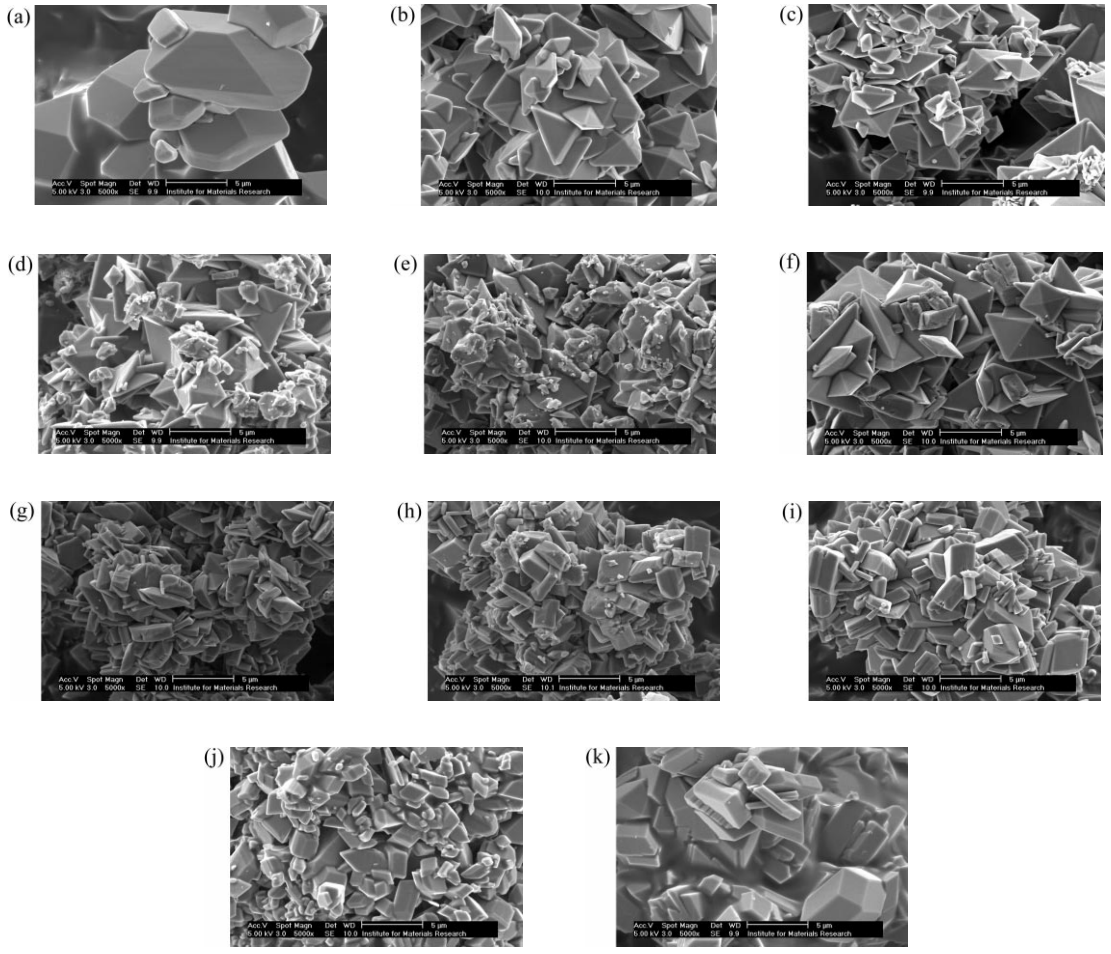

Fig. 3. SEM micrographs of the (co)precipitated samples: (a) sample 1; (b) sample 5; (c) sample 6; (d) sample 7; (e) sample 8; (f) sample 9; (g) sample 10; (h) sample 11; (i) sample 12; (j) sample 13; and (k) sample 3.

3.2. SEM-EDX analysis

3.2.1. Coprecipitates

Fig. 3 presents the morphology of the coprecipitates in relation to their stoichiometry. Since these coprecipitates, depending on their stoichiometry, have a crystal structure similar to $SrC_2O_4{\cdot}2.5H_2O$ and/or $CaC_2O_4{\cdot}H_2O$, the SE pictures of these single oxalates are also presented. $SrC_2O_4{\cdot}2.5H_2O$ (sample 1) is composed of octahedral crystals, as shown in Fig. 3(a). The SE pictures of samples 5, 6, 7, 8 and 9 (Fig. 3(b–f)) confirm that these samples are coprecipitates with Ca substitution in the lattice of $SrC_2O_4{\cdot}2.5H_2O$, since the octahedral crystals are still present. Secondary electron micrographs of sample 10 and 11 (Fig. 3(g) and (h)) show the presence of prism-like crystals, in addition to the still present octahedral crystals, confirming the presence of two phases, as already seen in the XRD patterns (Fig. 1(g) and (h)) of these samples. Finally, samples 12 and 13 show the same morphology (Fig. 3(i) and (j)) as $CaC_2O_4{\cdot}H_2O$ (sample 3, Fig. 3(k)), consisting of prism-like crystals.

Several EDX spot analyses on all the coprecipitated samples show that every crystal consists of both Sr and Ca, thereby confirming that homogeneous, intimately mixed oxalate powders are formed after synthesis.

3.2.2. Mechanical mixtures

Fig. 4 presents the SE micrographs of the single precipitated strontium oxalate (sample 2, Fig. 4(a)).

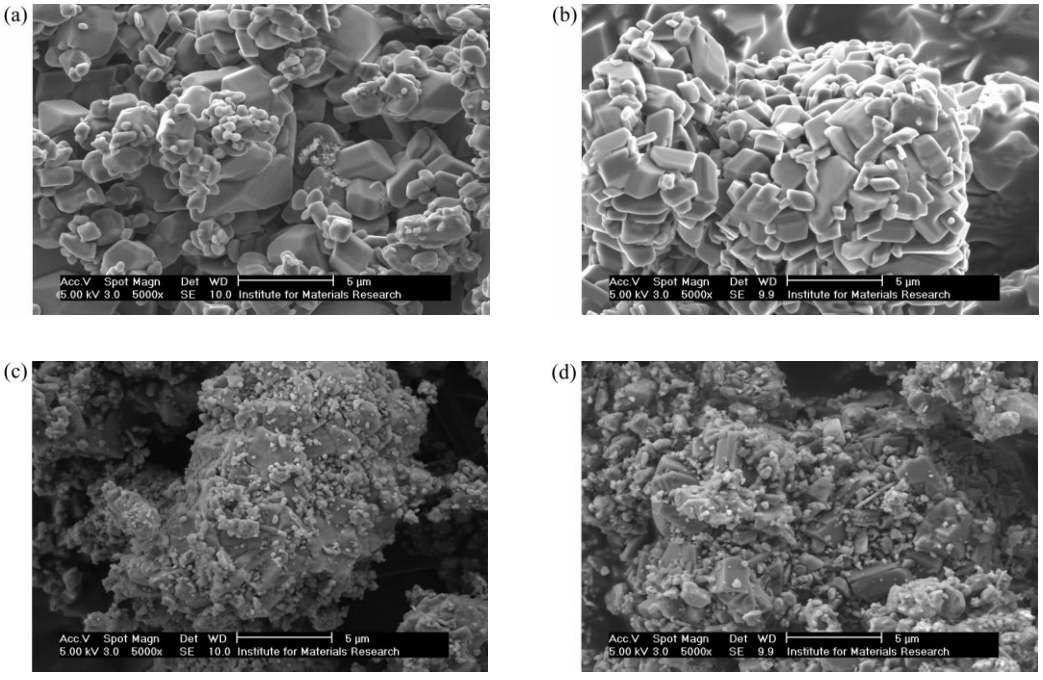

Fig. 4. SEM micrographs of individual oxalates and their mechanical mixtures: (a) sample 2; (b) sample 4; (c) sample 14; and (d) sample 15.

Comparison between Fig. 4(a) and Fig. 3(a) demonstrates clearly that sample 2 consists of two types of crystals: octahedral-like particles (comparable with the crystals in Fig. 3(a) and, therefore, most likely to correspond with the $SrC_2O_4{\cdot}2.5H_2O$ phase) and rounded particles. Calcium oxalate (sample 4, Fig. 4(b)) also contains two phases. Fig. 4(c) and (d) demonstrate the morphology of the two mechanical mixtures (samples 14 and 15). From EDX measurements it is confirmed that both Ca- and Sr-rich parts are present, confirming that the mixtures consist of separate grains of the starting materials. The morphology of the mixtures and the coprecipitates (Fig. 3(b), Fig. 4(c), Fig. 3(c) and Fig. 4(d)) confirm that the coprecipitates form highly homogenous powders.

3.3. Thermal analysis

In a previous report, the thermal decomposition of different forms of strontium oxalate in an inert atmosphere was studied [14]. Based on TG–EGA and DSC results, it was shown that $SrC_2O_4{\cdot}H_2O$ decomposes as follows:

1. endothermic dehydration between 130°C and 250°C;
2. endothermic formation of strontium carbonate between 420°C and 590°C with evolution of CO and CO_2 (formed by an exothermic disproportionation reaction); and
3. release of CO_2 during the endothermic formation of the oxide between 770 and 1020°C.

In the present study, we investigate the thermal decomposition behaviour of the individual precipitated oxalates, coprecipitates and mechanical mixtures. Table 2 presents a comparison between the experimental and theoretical percentage mass loss during each decomposition step of the single oxalates, coprecipitates and mechanical mixtures.

3.3.1. Coprecipitates

Fig. 5 presents the DTG curves of all the coprecipitated powders (samples 5, 6, 7, 8, 9, 10, 11, 12 and 13, Fig. 5(b–j), respectively) and the individual oxalates (samples 1 and 3, Fig. 5(a) and (k), respectively). The DTG curves of the coprecipitated oxalates are compared with those of the single oxalates in order to

Table 2
Comparison of experimental and theoretical % mass loss of single oxalates, coprecipitates and mechanical mixtures during their thermal decomposition

Sample	Dehydration/ %		Formation of carbonates/ %		Formation of oxides/ %	
	exp	theor	exp	theor	exp	theor
Strontium oxalate						
1	20.4	20.4	12.8	12.7	19.8	19.9
2	10.9	10.9	14.2	14.4	22.3	22.1
Calcium oxalate						
3	12.6	12.3	19.1	19.2	29.6	30.1
4	15.3	15.3	18.5	19.0	28.5	29.1
Coprecipitates						
	18.5	18.3	14.4	14.4	22.4	22.6
6	19.1	19.0	14.9	14.8	23.2	23.4
7	20.0	20.2	15.4	15.0	23.4	23.6
8	20.1	20.3	15.5	15.3	24.0	24.0
9	19.5	19.6	15.7	15.6	24.5	24.5
10	17.5	17.1	16.6	16.5	25.2	25.4
11	16.4	16.8	17.5	17.1	26.5	26.4
12	13.0	13.2	18.2	18.0	28.2	28.2
13	12.7	12.7	18.5	18.3	28.9	28.9
Mechanical mixtures						
14	12.2	12.2	15.8	15.7	24.0	24.1
15	12.7	12.7	16.2	16.3	24.7	25.0

explain the decomposition behaviour of the coprecipitates.

3.3.1.1. DTG results of the single oxalates: sample 1 and sample 3. The thermal decomposition of $SrC_2O_4{\cdot}2.5H_2O$ (sample 1) is illustrated in Fig. 5(a). The shape of the DTG curve between 50 and 200°C shows that the dehydration takes place in four steps. In the temperature domain between 400 and 490°C, the DTG curve shows one peak due to the decomposition of SrC_2O_4 into $SrCO_3$. The last DTG peak, between 680 and 900°C, corresponds to the formation of SrO.

The DTG curve of $CaC_2O_4{\cdot}H_2O$ (sample 3, Fig. 5(k)) reveals three peaks in the 100–160°C, 370–480°C and 520–690°C ranges which correspond, respectively, to water loss, formation of $CaCO_3$ and formation of CaO.

3.3.1.2. DTG results of the coprecipitated samples 5 and 6. Fig. 5(b) and (c) demonstrate the DTG curves of two $Ca_xSr_{1-x}C_2O_4{\cdot}yH_2O$ coprecipitates with x=0.35 (sample 5), x=0.49 (sample 6) and y=2 for both samples. The dehydration of both coprecipitates also takes place in four steps, but occurs at higher temperatures than the dehydration of $SrC_2O_4{\cdot}2.5H_2O$ (sample 1, Fig. 5(a)). The decomposition of the dehydrated oxalate powders takes place in one step, as demonstrated by the single DTG peak between 400 and 470°C in Fig. 5(b) and (c). This peak represent the formation of an intimately mixed $Ca_xSr_{1-x}CO_3$ intermediate, as described by reaction (1).

$$Ca_xSr_{1-x}C_2O_4 \rightarrow Ca_xSr_{1-x}CO_3 + CO \qquad (1)$$

The last DTG peak in Fig. 5(b) and (c) corresponds to the formation of CaO and SrO, respectively, as derived from the experimental percentage mass loss between 600 and 840°C (see Table 2, samples 5 and 6). The oxide formation thus takes place in one step according to reaction (2).

$$Ca_xSr_{1-x}CO_3 \rightarrow xCaO + (1-x)SrO + CO_2 \qquad (2)$$

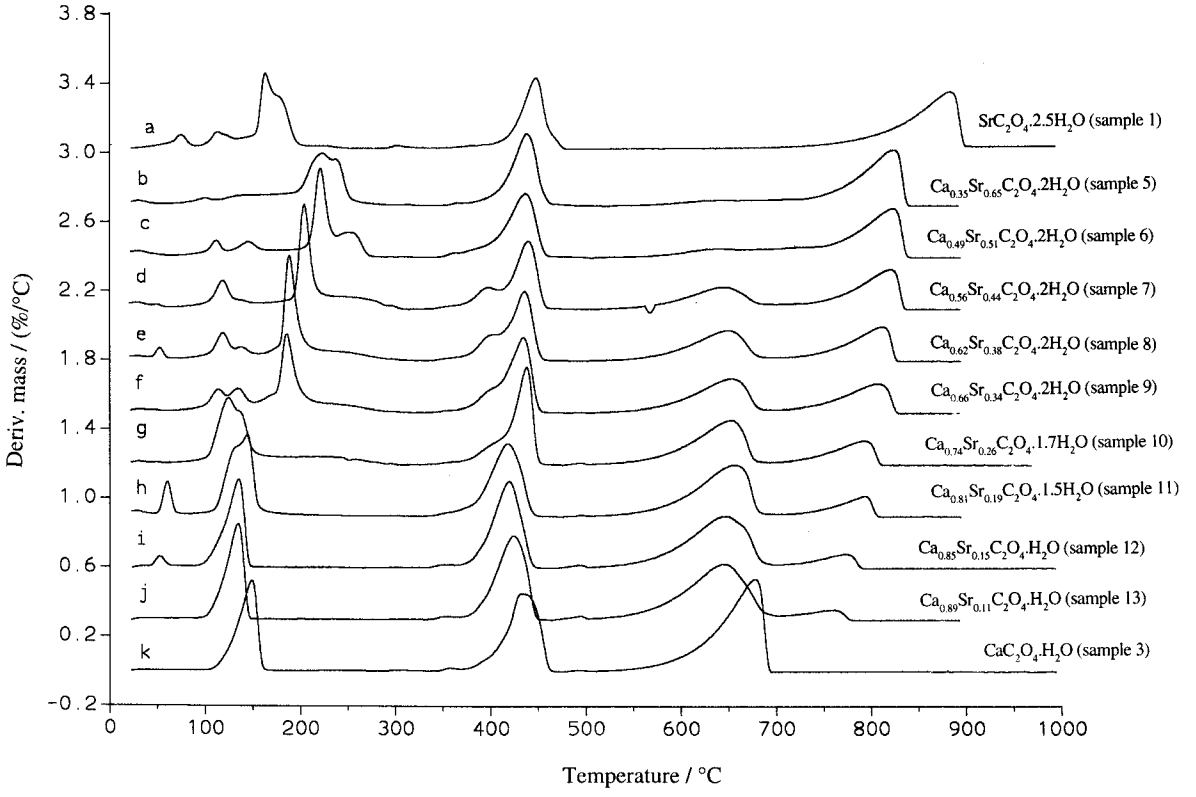

Fig. 5. DTG curves of the (co)precipitated samples: (a) sample 1; (b) sample 5; (c) sample 6; (d) sample 7; (e) sample 8; (f) sample 9; (g) sample 10; (h) sample 11; (i) sample 12; (j) sample 13; and (k) sample 3.

3.3.1.3. DTG results of the coprecipitated samples 7, 8, 9 and 10. Fig. 5(d–g) present the DTG curves of the $Ca_xSr_{1-x}C_2O_4{\cdot}yH_2O$ coprecipitates with x=0.56 and y=2 (sample 7), x=0.62 and y=2 (sample 8), x=0.66 and y=2 (sample 9) and x=0.74 and y=1.7 (sample 10), respectively. It is seen from these figures that the temperature region, in which the dehydration reaction takes place, is shifted to lower temperatures with increasing x values. Samples 7 to 9 have the same water content as samples 5 and 6. Presumably some vacancies occur in the predominantly $SrC_2O_4{\cdot}2.5H_2O$ lattice found for samples 5 to 9, equivalent to partial dehydration. The water content of sample 10 is situated between 2.5 and 1, which can be explained by the fact that a two-phase mixture of the $SrC_2O_4{\cdot}2.5H_2O$ and $CaC_2O_4{\cdot}H_2O$ lattices is found for this sample. The DTG curves of samples 7 to 10 (Fig. 5(d–g)) show two peaks, between 380 and 460°C, indicating that the decomposition of the anhydrous oxalate coprecipitates into carbonates takes place in two steps. The first step, between 380 and 410°C, can be attributed to the partial decomposition of the Ca–Sr oxalate into calcium carbonate (see reaction 3), followed by the decomposition of the remaining mixed oxalate into a homogeneous mixed Ca–Sr carbonate, between 410 and 460°C (see reaction 4). It can be concluded from these results that partial segregation during the decomposition process takes place. The following reactions describe the two-step decomposition of the anhydrous oxalate.

$$Ca_xSr_{1-x}C_2O_4 \rightarrow zCaCO_3 + Ca_{x-z}Sr_{1-x}(C_2O_4)_{1-z} + zCO \quad (3)$$

$$Ca_{x-z}Sr_{1-x}(C_2O_4)_{1-z} \rightarrow Ca_{x-z}Sr_{1-x}(CO_3)_{1-z} + (1-z)CO \quad (4)$$

The DTG peak, between 550 and 690°C (Fig. 5(d–g)), corresponds to the formation of CaO from $CaCO_3$ (see reaction 5). Finally, the mixed Ca–Sr carbonate is decomposed into CaO and SrO (see reaction 6) between 710 and 835°C as shown by the last DTG peak.

$$CaCO_3 \rightarrow CaO + CO_2 \quad (5)$$

$$Ca_{x-z}Sr_{1-x}(CO_3)_{1-z} \rightarrow (x-z)CaO + (1-x)SrO + (1-z)CO_2 \quad (6)$$

Table 2 (samples 7, 8, 9 and 10) shows a good agreement between the theoretical and experimental percentage mass losses for the complete decomposition of the oxalates into carbonates (reactions 3 and 4) and the formation of the oxides (reactions 5 and 6).

3.3.1.4. DTG results of the coprecipitated samples 11, 12, 13. Fig. 5(h–j) show the DTG curves of $Ca_xSr_{1-x}C_2O_4{\cdot}yH_2O$ coprecipitates with x=0.81 and y=1.5 (sample 11), x=0.85 and y=1 (sample 12) and x=0.89 and y=1 (sample 13). The water content of the three samples is removed at lower temperatures than for $CaC_2O_4{\cdot}H_2O$ (Fig. 5(k)). Sample 11 has an intermediary water content, as also seen for sample 10. Finally, samples 12 and 13 have the same water content as the $CaC_2O_4{\cdot}H_2O$ lattice. The dehydrated coprecipitates are decomposed into a mixture of two carbonates, between 370 and 450°C (see reaction 7). The complete segregation is confirmed by the good agreement between experimental and theoretical percentage mass loss for the separate formation of CaO and SrO (see reactions 8 and 9).

$$Ca_xSr_{1-x}C_2O_4 \rightarrow xCaCO_3 + (1-x)SrCO_3 + CO \quad (7)$$

$$CaCO_3 \rightarrow CaO + CO_2 \quad (8)$$

$$SrCO_3 \rightarrow SrO + CO_2 \quad (9)$$

3.3.2. Mechanical mixtures

Fig. 6 shows the DTG curves of the strontium oxalate sample 2, the calcium oxalate sample 4 and two mechanical mixtures of both oxalates (samples 14 and 15). In the 50–900°C range, the curves of the two mixtures (Fig. 6(c) and 6(d)) show seven peaks, which can all be assigned to the DTG peaks of the single

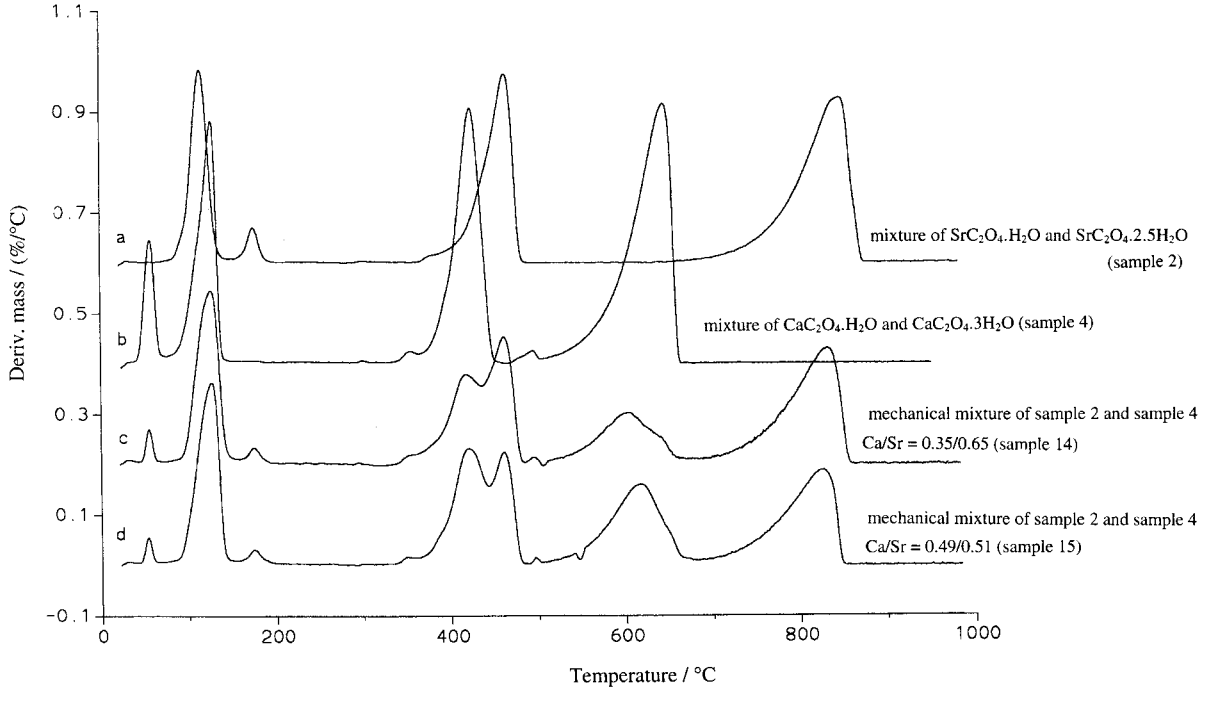

Fig. 6. DTG curves of individual oxalates and their mechanical mixtures: (a) sample 2; (b) sample 4; (c) sample 14; and (d) sample 15.

oxalates (Fig. 6(a) and (b)). The thermal behaviour of the mechanical mixtures is, hence, similar to that of the individual components.

The dehydration of the two mixtures takes place in three steps between 50 and 200°C. The decomposition of the anhydrous mixtures occurs in two steps between 350 and 500°C: DTG peaks 4 and 5 correspond, respectively, to the formation of $CaCO_3$ and $SrCO_3$. From a comparison with the pure oxalates (Fig. 6(a) and (b)), one can conclude that the DTG peak 6 between 550 and 700°C is due to the formation of CaO and that the final mass loss between 700 and 860°C (DTG peak 7) represents the formation of SrO.

4. Conclusions

It is concluded from XRD and SEM-EDX results that the coprecipitates form homogeneous solid solutions, unlike the mechanical mixtures of single oxalates, of which the crystal structure is preserved. Depending on the Ca/Sr stoichiometry, the coprecipitates consist of the lattice of $SrC_2O_4{\cdot}2.5H_2O$ and/or $CaC_2O_4{\cdot}H_2O$ in which partial substitution of Sr^{2+} by Ca^{2+} and Ca^{2+} by Sr^{2+} occurs. The coprecipitates with Ca/Sr ratios ≤ 1 decompose into an intimately mixed carbonate, unlike the equivalent mechanical mixtures, in which the oxalates decompose separately into their carbonates. Starting from Ca/Sr ratios >1, partial segregation occurs during the decomposition of the anhydrous coprecipitates into carbonates. Finally, it is demonstrated from TG results that complete segregation takes place during the decomposition of coprecipitates with Ca/Sr >4.

Acknowledgements

E. Knaepen is indebted to the "Vlaams Instituut voor de bevordering van het wetenschappelijk-technologisch onderzoek in de industrie (I.W.T)", Belgium, for financial support. M.K. Van Bael is a research fellow of the Fund for Scientific Research of Flanders (F.W.O Vlaanderen). The scientific responsibility of the contents of this paper is assumed by its authors. The authors wish to thank Christel Willems for the XRD measurements.

References

[1] D.W. Johnson, P.K. Gallagher, Ceramic Processing Before Firing, J. Wiley, New York, 1978, p. 125.
[2] A. Vos, J. Mullens, R. Carleer, J. Yperman, J. Vanhees, L.C. Van Poucke, J. Thermal. Anal. 40 (1993) 303.
[3] M.K. Wu, J.R. Ashburn, J.C. Torng, P.H. Hor, R.L. Meng, L. Gao, Z.J. Huang, Y.Q. Wang, C.W. Chu, Phys. Rev. Lett. 58 (1987) 908.
[4] C.J. Brinker, G.W. Scherer, Sol-Gel Science, Academic, London, 1990, p. 42.
[5] M.K. Van Bael, J. Mullens, R. Nouwen, J. Yperman, L.C. Van Poucke, J. Therm. Anal. 48 (1997) 989.
[6] S. Hoste, H. Vlaeminck, P.H. De Ryck, F. Persyn, R. Mouton, G.P. Van Der Kelen, Supercond. Sci. Technol. 1 (1989) 239.
[7] A. Vos, J. Mullens, J. Yperman, R. Carleer, J. Vanhees and L.C. Van Poucke, T.C. Krekels, G. Vantendeloo, F. Persijn, I. Vandriessche, S. Hoste, in: B. Raveau et al. (Eds.) Superconductivity, Technology Transfer Series, I.I.T.T.–T.C.M.A.S., Paris, 1991, p. 85.
[8] A. Vos, J. Mullens, R. Carleer, J. Yperman, L.C. Van Poucke, Bull. Soc. Chim. Belg. 101 (1992) 187.
[9] J. Mullens, A. Vos, A. De Backer, D. Franco, J. Yperman, L.C. Van Poucke, J. Thermal Anal. 40 (1993) 303.
[10] W.J. Scheule, J. Phys. Chem. 63 (1959) 83.
[11] S. Fischer, H. Langbein, C. Michalk, K. Knese, U. Heinecke, Cryst. Res. Technol. 26 (1991) 563.
[12] L. Walter-Levy, J. Laniepce, C.R. Acad. Sci. 257 (1963) 910.
[13] De Wolff, Technische Physische Dienst, Netherlands, JCPDS Grant-in-Aid-Report.
[14] E. Knaepen, J. Mullens, J. Yperman, L.C. Van Poucke, Thermochim. Acta 284 (1996) 213.